We are IntechOpen, the world's leading publisher of Open Access books Built by scientists, for scientists

6,900
Open access books available

185,000
International authors and editors

200M
Downloads

Our authors are among the

154
Countries delivered to

TOP 1%
most cited scientists

12.2%
Contributors from top 500 universities



WEB OF SCIENCE™

Selection of our books indexed in the Book Citation Index in Web of Science™ Core Collection (BKCI)

Interested in publishing with us?
Contact book.department@intechopen.com

Numbers displayed above are based on latest data collected.
For more information visit www.intechopen.com



Chapter 5

Application of Silver Nanoparticles for Water Treatment

Zenaida Guerra Que, José Gilberto Torres Torres,
Hermicenda Pérez Vidal,
María A. Lunagómez Rocha, Juan C. Arévalo Pérez,
Ignacio Cuauhtémoc López,
Durvel De La Cruz Romero,
Alejandra E. Espinosa De Los Monteros Reyna,
José G. Pacheco Sosa, Adib A. Silahua Pavón and
Jorge S. Ferráez Hernández

Additional information is available at the end of the chapter

http://dx.doi.org/10.5772/intechopen.74675

Abstract

In recent past development of silver nanoparticles and their application in the treatment of wastewaters is becoming a major area of research. It is mainly applicable to the removal of three major pollutants like pesticides, heavy metals, and microorganisms. Variety of synthesis techniques have been reported for preparation and characterization of silver nanoparticles. In our research, we synthesized Ag nanoparticles supported on ZrO_2 and ZrO_2-CeO_2 by a "deposit-precipitation method" as the first step and later sequentially synthesized Ag-Au supported on ZrO_2 and ZrO_2-CeO_2 by Redox method. Catalysts were evaluated in catalytic wet air oxidation (CWAO) of methyl tert-butyl ether and phenol. The CWAO is a liquid phase process for the treatment of organic pollutants operating at temperatures in the range of 100–325°C at 5–200 bar pressures. The selectivity and efficient of catalysts were evaluated by total organic carbon (TOC) and high-performance liquid chromatograph (HPLC). Ideally, the total mineralization of pollutants into CO_2 and H_2O is preferred.

Keywords: silver nanoparticles, wastewaters, catalytic wet air oxidation, phenol, MTBE

IntechOpen

© 2018 The Author(s). Licensee IntechOpen. This chapter is distributed under the terms of the Creative Commons Attribution License (http://creativecommons.org/licenses/by/3.0), which permits unrestricted use, distribution, and reproduction in any medium, provided the original work is properly cited. CC BY

1. Introduction

1.1. Refractory organic compounds in wastewater

Many factors have contributed to the deterioration of our environment, among them the exponential growth of the world population, the industrial sector excessive exploitation of the natural resources on earth, the generation of waste as a result of the activities by the aforementioned and the irrational consumption of the domestic sector. A large number of anthropogenic activities generate wastewater as a product of the processes that are carried out by the chemical, petrochemical, pharmaceutical, textile, agriculture and domestic sectors [1].

The conventional processes applied for water treatment have not been effective enough which can be evidenced worldwide showing that there are high concentrations of toxic, dangerous substances of the carcinogenic type, teratogenic and mutagenic, in surface and groundwater bodies of fresh water.

Freshwater is the most valuable resource we have since all the metabolic processes of the human body (reproduction, growth, development) are regulated by the presence of this fundamental substance. It is for these reasons that water pollution is a severe environmental problem, which is why strict water quality regulations have been implemented [2, 3].

In domestic, industrial, service or wastewater there are refractory organic compounds that by their chemical constitution are not susceptible to microorganisms in the aerobic digester to take advantage of it to obtain energy. Refractory molecules are organic compounds that are present in aqueous residues, formed by solid non-sedimentable particles of colloidal size, which as they are not biodegradable or even toxic thus cannot be treated by conventional methods since they show resistance to biological degradation from microorganisms, therefore, after the application of conventional treatments, remain present [4, 5]. These organic compounds tend to resist conventional methods of wastewater treatment [6]. The current conventional technologies available for wastewater treatment, whose processes can be physical, chemical and biological are very diverse and have been used to remove aqueous pollutants [7].

In general, conventional processes are frequently classified as preliminary, primary, secondary (biological) and tertiary treatments. Specifically, the biological treatment is designed to eliminate the dissolved organic load of the waters using microorganisms. The microorganisms used are responsible for the degradation of organic matter. The aerobic treatment of wastewater converts organic pollutants into wastewater in a good amount of excess sludge and oxidizes the remainder with oxygen to carbon dioxide [8, 9]. The treatments depend on the aerobic or anaerobic organics, for example, the *Ochrobactrum cytisi* is an aerobic bacterium used to degrade methyl tert-butyl ether (MTBE). In the aerobic mechanism, oxygen is essential for successful operation of the systems [10].

In most applications of conventional wastewater treatment, the complete oxidation of organic pollutants to carbon dioxide and water is difficult to achieve due to the formation of even more refractory intermediates such as short chain carboxylic acids. As a consequence, the combination of processes has a great potential benefit, chemical treatment of advanced oxidation (unconventional) and then the conventional biological that could be a more efficient way

to reduce pollution; this has been presented as a strategy. For such a case, chemical oxidation is needed to destroy persistent molecular structures, remove high ecotoxicity and improve solubility in water [9, 11].

1.2. Environmental impact of refractory organic compounds

The persistent or refractory organic pollutants, such as phenols and derivatives, polycyclic aromatic hydrocarbons (PAHs), polychlorinated by phenyls (PCBs), pesticides or even other organic compounds, are very slowly metabolized or otherwise degraded. Since long, plant protection products, substituted phenols, non-biodegradable chlorinated solvents, PAHs, PCBs, and surfactants are recognized as examples of relevant substances, because of the environmental damage they cause [2, 7].

The Phenol and phenolic compounds are harmful from the human health; they can cause tissue detachment, necrosis, digestive delay, kidneys and liver damage. Furthermore, if the discharge is at very low concentrations, they are highly dangerous to aquatic life and transfer a particularly unpleasant smell and taste [9, 12]. MTBE is a suspected human carcinogen by the US Environmental Protection Agency, which is hazardous to human health [10]. Therefore, it is essential to treat water contaminated properly with refractory organic compounds before being discharged to freshwater bodies.

1.3. Non-conventional treatment for the degradation of refractory organic compounds

The unconventional treatment methods include membrane separation, adsorption by activated carbon, the Fenton Process, oxidation using H_2O_2/UV, advanced oxidation processes (AOPs) and chemical oxidation technologies. The environmental technologies play an important role in de-coupling environmental from economic growth. Advanced treatment technologies have been demonstrated to remove various potentially harmful compounds that could not be effectively removed by conventional treatment process [8, 9, 13, 14].

The objective of oxidative treatment processes is frequently to rapidly convert organic molecules to carbon dioxide, water, and innocuous products by exploiting chemical principals in order to surmount the kinetic restraints, which are responsible for the slowness of some of the reactions. AOPs have been roughly defined as near ambient temperature treatment processes based on highly reactive radicals, especially the hydroxyl radical (.OH). The .OH radical is among the strongest oxidizing species used in water and wastewater treatment and offers the potential to greatly accelerate the rates of contaminant oxidation. The generation of OH, radicals are commonly accelerated by combining ozone (O_3), hydrogen peroxide (H_2O_2), titanium dioxide (TiO_2), heterogeneous photocatalysis, UV radiation, ultrasound, and (or) high electron beam irradiation [15].

Besides, the Catalytic Wet Air Oxidation process (CWAO) has been adopted for wastewater with very low concentrations of contaminants that cannot be incinerated or very high concentrations that cannot be biologically treated. The main efforts in research are frequently directed to reach the total oxidation of organic effluents in wastewater under less severe conditions in the presence of homogeneous or heterogeneous catalysts [16, 17].

CWAO is regarded one of the most important industrial processes to destroy hazardous, toxic and non-biodegradable organic compounds present in wastewater streams. The process involves the use of a trickle-bed or slurry reactors operating at temperatures in the range of 100–325°C at 5–200 bar pressures, with oxygen as oxidant agent, using a supported catalyst [18–20].

1.4. Silver nanoparticles supported applied in the degradation of organic matter

Currently, efforts have been directed to conduct studies of silver nanoparticles (NPS) in organic matter oxidation due to the persistence of certain molecules after conventional degradation treatments, or to their partial oxidation to obtain precursors for other valuable products in the industry.

Noble metals have been widely used in the CWAO of model compounds, as well as in real wastewater due to their excellent catalytic activities. One of these metals is the finely dispersed nanometer-sized silver particles that have been studied by various authors, as an ideal feature for outstanding catalytic properties [21–24].

Metal nanoparticles have been widely studied because they have excellent optical, mechanical, electrical, magnetic, and chemical properties. These properties are generally the product of the large surface area possessed by the nanoparticles due to the reduction in size. Recently, metallic nanoparticles have turned out to be very attractive for their commercial development, which is why their production has increased in different industries such as aeronautics, agriculture, food, automotive, biomedical, cosmetic, pharmaceutical, computer, textile, catalysis, among others [25, 26].

Metals such as gold, silver, palladium, and copper are used for the manufacture of nanoparticles of different shapes and sizes. The techniques and conditions when the synthesis is performed the nanoparticles are directly influenced by the morphology and physical–chemical properties of these. Of all the metal NPS, in this chapter, we will discuss silver and gold for their catalytic application.

2. Silver nanoparticles supported on metal oxides for the catalytic wet air oxidation of refractory organic compounds

The technology used for the mineralization of refractory organic matter, has different types of treatments, which we will discuss this chapter, it will be focused on the CWAO, which is based on a reaction in the presence of oxygen on the problem molecule (phenol, MTBE) in which is used inorganic catalysts, at a certain pressure and specific temperature, with the aim of the total or almost total degradation of the pollutant.

2.1. Silver nanoparticles supported applied in the degradation of organic matter

Organic matter is composed mainly of proteins, carbohydrates, and fats, biodegradable organics measured in terms of biochemical oxygen demand (BOD) and chemical oxygen demand

(COD). If there is untreated discharge to the environment, its biological stabilization can cause the depletion of natural oxygen sources and the quality of fresh water in available sources [9].

The silver nanoparticles, in particular, are exceptional due to their excellent optical, thermal, catalytic, electromagnetic, adsorbent and antimicrobial properties, which differ greatly to the properties that silver presents in volumetric sizes. This is due to the reduction in size which produces an increase in the surface area in relation to the volume, as well as the shape of the nanoparticle [27–30]. The optical properties of nanoparticles strongly depend on the particle size and the refractive index of the medium. The dependencies of these properties with respect to particle size can be of two kinds, due to the increase in energy caused by the quantum confinement of the system or by the resonance of the surface plasmon [30, 31]. The surface plasmons are defined as the collective oscillation of conduction electrons on the surface of the particle, as a result of the interaction with the electric field of electromagnetic radiation [31, 32].

2.2. Au-Ag bimetallic nanoparticles supported in oxide

The supported bimetallic gold-silver nanoparticles have been reported in various reactions of CO oxidation, photoreaction of phenol degradation among others. In addition to the chemical relationship between the metals, the proportions of the mesoporous support in the case of mixed oxides have a remarkable effect on the catalytic activity [33–37]. Many experiments show that the modification of the structure of the support surface or the morphology can result in the improvement of the catalytic activity in case of the oxidation of CO [34, 38]. Modifying nanoparticle systems with such characteristics are procedures that require a deep study of the physicochemical properties of the materials in question, Au-Ag nanoparticle alloys which is a system that is currently studied for oxidation systems and has peculiarities that are of special scientific attention For example, particle size no longer plays a key role in the determination of catalytic activity, while the composition of the Au:Ag ratio becomes important [34]. However, this type of mixed nanoparticle has been studied as "inert" systems and it is not clear how it affects the support in the alloy particle, size and catalytic activity [37].

That is why our research group was interested in working with noble metals (Ag, Au) and evaluating them in CWAO, since it has been little studied, despite its interesting properties in catalytic oxidation. Next, we present the most relevant synthesis methods, results and conclusions of Ag and Au-Ag nanoparticles supported on ZrO_2 and ZrO_2-CeO_2 for the degradation of phenol and MTBE.

3. Synthesis, characterization and catalytic activity of silver nanoparticles

The NPS of Ag^0 can be manufactured using a large number of methods such as electric, chemical reduction, photochemistry, among others [39]. The reduction technique is the most economical and used method due to its large-scale manufacturing and easy handling [40–42].

From these methods, our research group decided to carry out different strategies: (1) sol–gel method to obtain simple (ZrO_2) and mixed (ZrO_2-CeO_2) supports, (2) deposit-precipitation with NaOH for the synthesis of NPS of Ag, (3) with urea to obtain the bimetallic materials, (4) sequential deposit precipitation method to introduce the Au and obtain the bimetallic (Au-Ag), and (5) oxide-reduction method to introduce a second metal (Au) and obtain bimetals. The materials were evaluated in the catalytic activity using probe molecules: phenol and MTBE.

3.1. Synthesis of silver monometallic catalysts for deposition-precipitation using NaOH

Brackets of simple zirconium oxides (Zr) and mixed oxides (Zr-Ce) were initially prepared by the sol-gel method. After addition of the metal (Ag) by the deposition-precipitation method which is a modification of the precipitation methods in solution. It consists of the conversion of a highly soluble metal precursor into another substance of low solubility, which precipitates specifically on the support and not in the solution [43].

3.2. Synthesis of Au-Ag bimetallic catalysts for sequential deposition-precipitation using urea

The materials that were synthesized have a 1:1 molar ratio of Ag:Au.

The addition of the second metal (Au) was done by the deposit-precipitation method, with a slight modification to the synthesis process, this is because the second metal is gold, these gold nanoparticles are very sensitive to the preparation method, the choice of the support or the treatment conditions, for which the deposit-precipitation process with urea was chosen [44].

At the end of the synthesis of the catalysts, materials with a weight concentration of 1.4% silver supported in the oxides were obtained.

3.3. Synthesis of Au-Ag bimetallic catalysts by recharge or redox

The selective deposition of Au on the surface of nanoparticles of a primary oxide-supported metal has been performed by a redox method that is based on the reduction of the second metal ions with hydrogen adsorbed on the surface of first metal or with itself [45].

The bimetallic catalysts were prepared by the recharge method, reducing $HAuCl_4^-$ (from $HAuCl_4$) with pre-adsorbed hydrogen on the silver surface. An amount of 2 g silver monometallic catalyst supported on zirconia and mixed oxides of pre-reduced zirconia-ceria was introduced into a reactor under nitrogen flow and was activated at 400°C for 1 h under a hydrogen atmosphere. Next, the solution of the gold precursor, previously degassed under a stream of nitrogen, was introduced onto the catalyst, taking an amount sufficient to synthesize a 1:1 molar ratio. After a reaction time of 1 h under hydrogen bubbling at room temperature, the bimetallic catalyst is dried with hydrogen at room temperature, then at 100°C (heating rate 2°C/min) overnight. Finally, the five bimetallic catalysts synthesized were reduced under a stream of hydrogen at 400°C for 1 h, with a heating rate of 2°C/min [45–47].

3.4. Degradation of pollutants (methyl tert-butyl ether and phenol) by catalytic wet air oxidation over Ag/ZrO_2-CeO_2

All catalysts were tested in a high-pressure stainless steel batch reactor (Parr Instruments) equipped with sampling valve, magnetically driven stirrer, gas supply system and temperature controller. The Catalytic Wet Air Oxidation reaction was carried out as follows: using a reaction volume of 300 mL of an aqueous solution with a concentration of 440 ppm and 1 g/L of the monometallic catalyst. After the reactor was heated at 100°C to reach the desired temperature, pure oxygen (O_2) at 8 bar was added under stirring. The catalysts were previously reduced at 400°C during 3 h with an H_2 flow (60 ml/min). The reaction was performed for 60 min. The samples in the effluent were taken at intervals of 10 min through 1 h, and the MTBE content (C), intermediate content and Total Organic Carbon (TOC) were analyzed. MTBE content and intermediate content were measured with High-Performance Liquid Chromatograph (HPLC). Total Organic Carbon (TOC) of the samples was measured with a TOC 5000 Shimadzu Analyzer. The conversion of MTBE and phenol, respectively, for the different materials and the TOC was calculated using:

$$X_{pollutant} = \frac{C_0 - C_{60}}{C_0} \times 100\%$$

$$X_{TOC} = \frac{TOC_0 - TOC_{60}}{TOC_0} \times 100\%$$

where TOC_0 is Total organic carbon at t = 0 (ppm), C_0 is the MTBE or Phenol concentration at t = 0 (ppm), C_{60} is the MTBE or Phenol concentration at t = 1 h of reaction (ppm), TOC_{60} is total organic carbon at t = 1 h of reaction (ppm). So the selectivity was calculated according to following equation [48].

$$S_{CO_2} = \frac{X_{TOC}}{X_{mtbe}} \times 100$$

The initial rate (r_i) was calculated from the MTBE or phenol conversion as a function of time, using the following equation:

$$r_i = \left(\frac{\Delta_{mtbe}(\%)}{\Delta t\, m_{cat}}\right)\left([pollutant]_i \right.$$

where $\frac{\Delta_{mtbe}(\%)}{\Delta t}$, $\frac{\Delta_{phenol}(\%)}{\Delta t}$ is the conversion at initial time; $[pollutant]_I$ = initial concentration of the pollutant and m_{cat} = mass of catalyst ($g_{cat}L^{-1}$).

3.5. Characterization of monometallic nanoparticles (Ag) y bimetallic of Au-Ag supported on Simple and mixed oxides of ZrO_2 and ZrO_2-CeO_2

In **Table 1** the materials studied are listed, the nomenclature is Ag/ZrO_2-Cex and Au-Ag/ZrO_2-Cex, where X = % cerium.

Nomenclature	Supports and catalysts	Synthesis method					Molecular probe	
		Sol–Gel	Deposit-precipitation			Redox method		
			NaOH	Urea	Urea: sequential		MTBE	Phenol
	Supports							
S1	ZrO_2	x						
S2	ZrO_2-Ce0.5	x						
S3	ZrO_2-Ce1	x						
S4	ZrO_2-Ce5	x						
S5	ZrO_2-Ce10	x						
S6	ZrO_2-Ce15	x						
S7	ZrO_2-Ce20	x						
	Monometallic							
M1	Ag/ZrO_2		x				x	x
M2	Ag/ZrO_2-Ce0.5		x					x
M3	Ag/ZrO_2-Ce1		x					x
M4	Ag/ZrO_2-Ce5		x				x	x
M5	Ag/ZrO_2-Ce10		x				x	x
M6	Ag/ZrO_2-Ce15		x				x	x
M7	Ag/ZrO_2-Ce20		x				x	x
	Bimetallic							
B1-U*	Au-Ag/ZrO_2			x	x			x
B2-U*	Au-Ag/ZrO_2-Ce0.5			x	x			x
B3-U*	Au-Ag/ZrO_2-Ce1			x	x			x
B4-U*	Au-Ag/ZrO_2-Ce5			x	x			x
B5-U*	Au-Ag/ZrO_2-Ce10			x	x			x
B6-U*	Au-Ag/ZrO_2-Ce15			x	x			x
B7-U*	Au-Ag/ZrO_2-Ce20			x	x			x
B1-R*	Au-Ag/ZrO_2					x	x	
B2-R*	Au-Ag/ZrO_2-Ce5					x	x	
B3-R*	Au-Ag/ZrO_2-Ce10					x	x	
B4-R*	Au-Ag/ZrO_2-Ce15					x	x	
B5-R*	Au-Ag/ZrO_2-Ce20					x	x	

S = supports (1–7), Mx = monometallic, By-U* = bimetallic from urea y Bz-R = bimetallic by the redox method. x = 1–7, y = 1–7, z = 1–5.

Table 1. Method of synthesis of Ag and Ag-au/ZrO_2-Cex, and catalytic evaluation: phenol and MTBE.

The real properties were determined by the Brunauer-Emmett-Teller method (BET) and the average pore diameter was estimated by the BJH method. The real values of the supports (S1 and S7) indicate that the specific area did not vary significantly (S_{BET} 72–63 m^2/g) when increasing the cerium content and the average pore diameter was 3.6 and 3.3 nm. When depositing Ag (M1 and M7) it was 68 and 49 m^2/g, respectively, and, with Au, samples B1 and B7 were 69 and 62 m^2/g. There are no significant changes in these properties in the synthesized materials. All the isotherms were of the type IV characteristics of well-defined mesoporous systems. The shape of the hysteresis loop was H_2 type according to the IUPAC classification. All materials have a unimodal pore size distribution.

In the X-ray diffraction patterns (XRDs) of the supports (**Figure 1**), diffraction planes (101), (110), (112) and (211) are observed, having as the main peak the plane (101) located at 30.11° on a 2θ de scale; these planes are characteristic of the tetragonal phase of ZrO_2 with a spatial group of *P42/nmc* and reported cell parameters of a = b = 3.612 Å and c = 5.212 Å and angles for $\alpha = \beta = \gamma = 90°$ [49].

As the concentration of ceria increases in the surface of ZrO_2 it stabilizes the tetragonal phase of it and this is easily appreciated when taking as reference the material Au-Ag/ZrO_2 in which a small peak is observed in 28.41° in 2θ, characteristic of the monoclinic phase of ZrO_2 [50], this peak disappears in the materials synthesized with a concentration of 5% CeO_2 (Au-Ag/ZrO_2-Ce5) at 20% CeO_2.

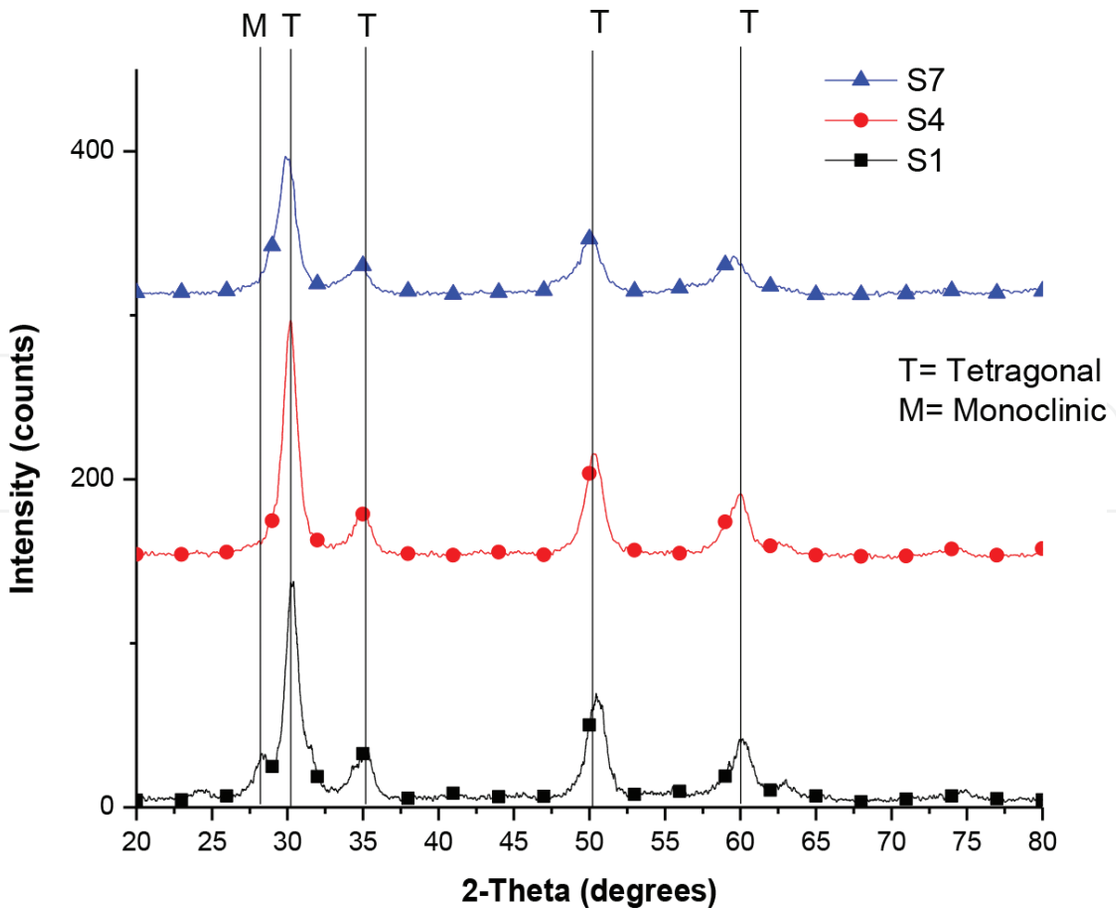


Figure 1. X-ray diffraction pattern of S1, S4 and S7 supports.

The average crystal size was calculated using the Scherrer equation [51]. The results indicate that the crystal average decreased when CeO_2 of 9.50 nm was added in ZrO_2 at 8.36 nm in ZrO_2-Ce0.5 and, 6.33 nm in ZrO_2-Ce20 (S7). When the Ag was supported in these materials values of 8.36, 8.04 and 6.52 nm were recorded in Ag/ZrO_2, Ag/ZrO_2-Ce0.5 and Ag/ZrO_2-Ce20, respectively, and, when introducing the second metal (Au) in these bimetallic materials the values were as follows: 9.09, 8.36, and 6.33 nm. The estimated average crystallite size varies depending on the concentration of cerium in the structure of ZrO_2 in the case of supports, but changes when depositing the Ag on the surface of the material, the smaller average size of the crystal was for the materials S7, M7, and B7. In the bimetals (Au-Ag) the size of the crystallites does not vary much in relation to the supports. If they are of a larger size, they decreased in size, this is due to the sequential precipitation deposition method, which not only deposits the second metal (Au) in the system's matrix but also redisperses the entire system, recovering the crystal size of the support.

The crystalline phases of the support (S1–S7) and the monometallic catalysts (M1–M7) are similar, and there are no differences in the diffraction peaks (**Figure 2**), so the amount of Ag that was deposited on the support formed no agglomerations of the metal, forming silver nanoparticles well dispersed in the material, this is corroborated by the UV-Vis with DRS (surface plasmon) and the TPD of H_2 of the materials.

In the XRD diffractograms of the bimetallic materials (**Figure 3**), a small peak could be observed at 38.33° in 2θ, attributed to the diffraction of silver or gold, of which the two elements have

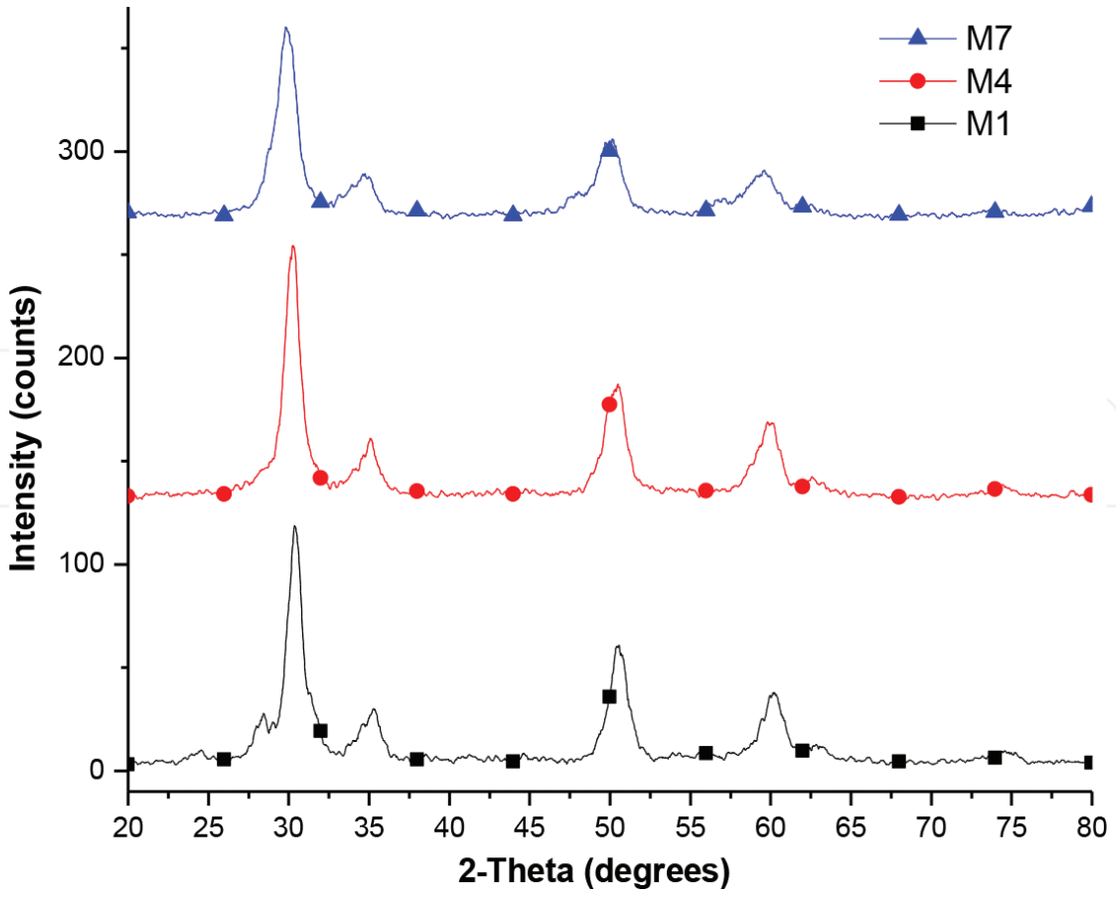


Figure 2. X-ray diffraction of M1, M4 and M7, monometallic catalysts.

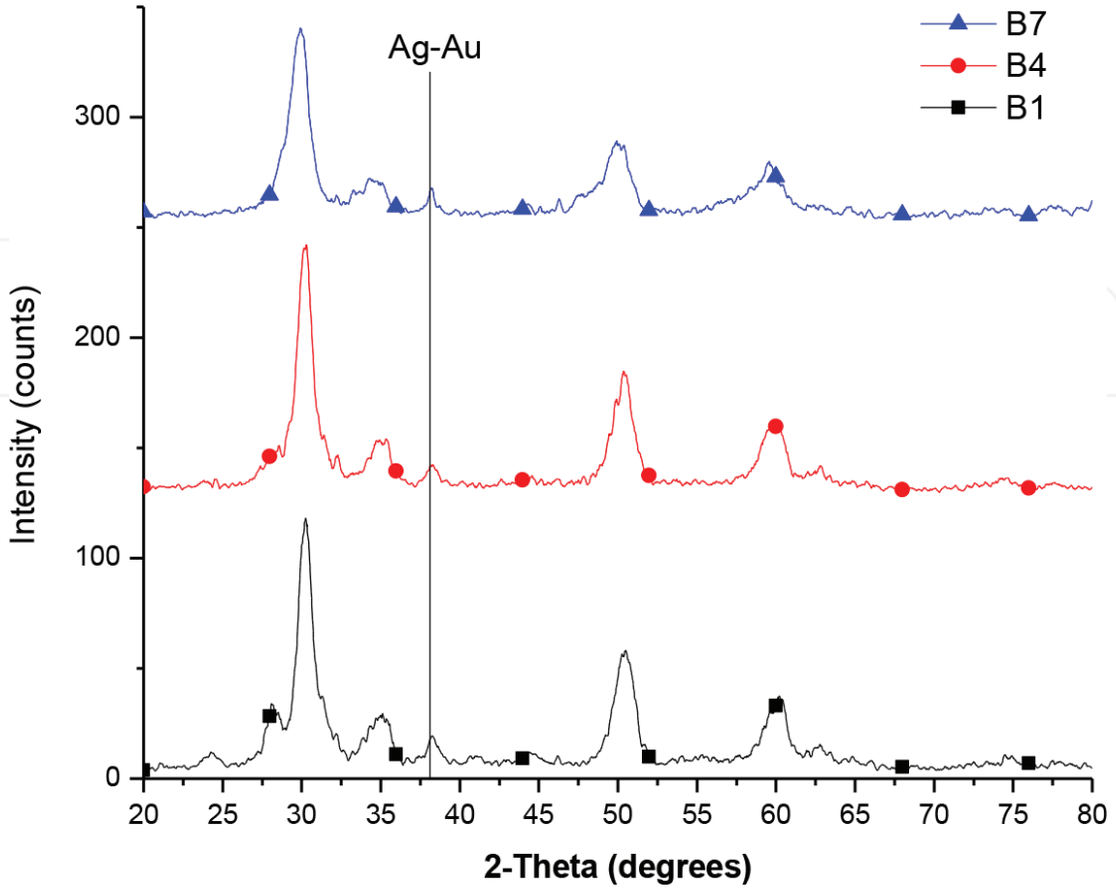


Figure 3. X-ray diffraction pattern of B1, B4 and B7, bimetallic catalysts.

diffraction peaks in the same region due to having a similar crystalline structure (fcc, cubic centered on the faces). Since the concentration of silver is relatively low (1.4% by weight), the equipment does not detect peaks in the DRXs in the monometallic, but when depositing the gold 1:1 molar, the concentration of the metals together reaches ~4% by weight.

Below are the TPD of H_2, TPD-NH_3, and TPR-H_2

3.5.1. H_2 of TPD

The accessibility of the silver and silver-gold catalysts was determined from the thermogram area of the H_2 of TPD, assuming a stoichiometry H:Ag = 1 and H:Au = 1 [52]. The TPD-H_2 method allows the calculation of the dispersion of the metal deposited on the surface of the support, as well as an estimate of the average size of the metallic crystals on the surface.

The values of percent dispersion and average crystal size for the monometallic and bimetallic catalysts prepared on the ZrO_2 carriers modified with ceria are presented in **Table 2**.

The dispersion percentage of the monometallic materials M1, M4 and M7, increases as the aggregate of cerium increases in the ZrO_2 surface of 26 > 28 > 80%, which indicates a better dispersion of the silver promoted by this promoter, and smaller sizes of metallic glass for the M7 monometallic catalyst. Bimetallic catalysts (B1, B4, B7) tend to increase in size, which is expected when a second metal is deposited on the surface, but this does not occur in material

Catalyst	μmol of H_2/g catalyst	TPCM (nm)*	%D**
M1	34	7.3	26.2
M4	37	6.7	28.5
M7	104	2.4	80.1
B1	37	9.1	14.8
B4	169	2.0	67.5
B7	29	11.6	11.6

*TPCM = Average size of metallic crystallite**%D = dispersion percentage.

Table 2. Monometallic catalysts (M1, M4, and M7) and bimetallic catalysts (B1, B4, and B7): μmol H_2/g, average crystal size, and dispersion percentage.

B4 where it decreases possibly due to the strong metal support interaction that exists to that concentration of ceria in the material. As it was observed in the maximum desorption temperature that was of 366°C for the material B1, on the other hand in the material B4 it is of 446° C followed by a peak at 256°C.

The B7 material increases its average size of metallic crystal in relation to its monometallic counterpart (M7) and presents peaks of desorption at 423°C followed by one at 294°C which suggests very strong interactions between the support and the metals deposited in its surface.

3.5.2. NH_3 of TPD

This technique is used in catalysis to determine the number and type of acidic sites available on the surface of the catalyst. Desorption at a programmed temperature of ammonia is based on the chemisorption of a gas on a solid and the subsequent desorption of that gas by a progressive increase in temperature.

Monometallic materials show some acidity, but the most notable is M7, which presents ammonia desorption peaks at a temperature of 435°C and is due to strong acid sites; the percentage of acidity of the sites have 69.9% for strong acid sites. In the case of bimetallic catalysts, the deposit of Au on the surface of the monometallic material changes the acidity of M4 to desorption sites of a higher temperature for the case of its bimetallic counterpart B4.

For bimetallic materials, the appearance of strong acid sites is due to the deposition of the second metal to the surface of the monometallic material. The addition of second metal (Au) can modify the active sites of mono-metallic material. This change can be shown through TPD-NH_3 when increasing the number of moderate and strong acid sites. An alternative modification can be done through addition of promoter CeO_2 in the support. In this study we synthesized supports with different CeO_2 content, increasing gradually when ceria is present in high concentration enhance strong metal-support interaction effect.

It has been reported that the addition of Au by the precipitation deposition method increases the oxygen reducibility of ceria [52]. In general, the capacity to store oxygen of the systems

containing CeO_2 results from the change in the associated oxidation state that is reversible in the case of materials with Ceria in a very general way is $2CeO_2 \leftrightarrow Ce_2O_3 + ½\ O_2$ [53], so that denotes the importance of the oxygen kinetics incorporated or removed from the CeO_2 structure promoted by the Au is a crucial step in the formation of stronger acid sites.

3.5.3. H_2 of TPR

The studies of the programmed temperature reduction were made to the materials M7, B7, M4, and M7. In B7 material, two reduction peaks predominate, one at 130° C and the other at 200°C corresponding to the metal on the surface of the material, because there are oxidized species of silver (AgO and Ag_2O) and Gold (Au_2O and Au_2O_3) in The surface of the metal will be reduced to the aforementioned temperatures. Another peak that is observed is at 275°C which may be due to the reduction of the Ag_2O on the surface of the support, this peak of reduction indicates that on the surface of the support the silver is oxidized easily due to the strong interaction with CeO_2, in the literature it is indicated that the ceria is reduced at two temperatures 770 and 1100 K [54], not appearing in the ranges of analysis of the samples, this is corroborated by UV-Vis and TPD of H_2. Associated with the small cerium crystal and its reduction temperature, it is clear to note that this helps the material to have a better oxidation–reduction on the surface contributing oxygen to the system and increasing its catalytic activity.

The monometallic materials are easily oxidized even after the thermal treatment with Hydrogen, where two reduction peaks are shown at 66 and 158°C for the M7 material. The peaks of the silver as the support without Ceria (material M1) in relation to those that do have the promoter, present peaks at lower temperatures than for the monometallic ones.

3.6. Catalytic evaluation (phenol, MTBE)

3.6.1. Phenol

In the group of M catalysts the best nanomaterial was M7 which corresponds at Ag/ZrO_2-Ce20 for degradation of phenol. The conversion of phenol was followed through Gas chromatography and Total Organic Carbon. M7 has 30% of conversion of phenol and 25% of TOC. The rest of the M catalyst has lower values. The reasons for this behavior are explained basically through TPD-NH_3. M7 has a higher percentage of strong acid sites than the rest of his other counterparts. M7 has 69.9% of strong acid sites and M4 and M1 0%. As they know the adsorption of molecules over a strong acid site is more stable than the adsorption over a weak acid site.

In the group of B-U* catalysts the best nanomaterial was B7 which corresponds at Ag-Au/ZrO_2-Ce20 for degradation of phenol. The conversion of phenol was followed through Gas chromatography and Total Organic Carbon. B7 has 61% of conversion of phenol and 40% of TOC. The rest of the B-U* catalyst has lower values. The reasons for this behavior are explained basically through TPD-NH_3. M7 has a higher percentage of strong acid sites than the rest of his other counterparts. B7 has 47.9% of strong acid sites and B4 35%. As they know the adsorption of molecules over a strong acid site is more stable than the adsorption over a weak acid site. Thus, the bimetallic catalyst B7 overcomes the monometallic catalyst M7. Therefore it is the most active for CWAO reaction of phenol, mineralizing intermediaries in a more efficient way.

The B7 catalyst showed the highest conversion of all the catalysts. B7 has 61% of conversion of phenol and 40% of Total Organic Carbon (TOC), which is highly consistent with the accessibility data for the Ag-Au active sites obtained by the acidity study obtained by TPD-NH_3, in which this catalyst presented the values higher in the percentage of strong acidity. When Au is added to the solid, the conversion of the model molecule increases in the case of the M4 and M7 catalysts. However, catalyst M1 decreased its catalytic activity by depositing gold (material B1) and had greater selectivity to CO_2 production. The bimetallic catalyst B7 prepared by the sequential deposition-precipitation technique has the highest conversion (61%) compared to the catalyst B1 (16%). In catalyst B7 there is a higher conversion of phenol and the highest selectivity to CO_2. Therefore, the increase in oxidation and conversion to CO_2 can be explained by an adequate relationship between the acid function of the support and the metallic function of the system.

3.6.1.1. Degradation of phenol (TOC)

The results of metallic dispersion of the monometallic materials (M1-M7) indicate a decrease in the average crystal size in relation to the increase in Ceria concentration. Despite the size, it was not a determinant factor in the degradation, where the monometallic M4 (6.7 nm) has higher conversion than the M7 (2.4 nm). The deposit of the gold to the monometallic catalyst increases the crystal size and increases the degradation of the phenol for the catalyst (B7). It was observed that the increase in the degradation and mineralization of phenol due to the addition of gold to the system promotes the oxidation change of CeO_2, causing structural and electronic defects in bimetallic materials. This is also corroborated in the analysis of the acidity in the material.

The increase in the activity promoted by gold in the catalysts with a greater amount of ceria shows that gold facilitates the reduction of CeO_2, causing superoxide species in the surface and increases the oxidative-reductive capacity of the promoter. Various authors [38, 51, 55] have studied the alloy of Ag-Au in catalytic reactions, and have proposed that the natural adsorption of oxygen by silver is favored by the presence of gold. This implies that the adsorption of oxygen and its subsequent activation by gold creates superoxide species (O_2) on the surface of the bimetallic nanoparticles; which, besides being catalytically active, have a strong metal-support interaction, which favors the catalytic activity.

3.6.2. MTBE

Results from Ag/ZrO_2-CeO_2 catalysts with 5, 10, 15 and 20% ceria the MTBE conversion has values between 52 and 90%, being the Ag/ZrO_2-Ce15 catalyst the most active with 90% MTBE conversion.

In TOC conversion for monometallic catalysts (**Figure 4**) it is strongly distinguished the effect of ceria dopant on the conversion of intermediates, because at a high content of cerium oxide (15–20%) it results in high percentages of TOC conversion (69 and 80%), so the reaction rate is faster for the conversion of intermediates and therefore, the concentration of the intermediate compounds is degraded more efficiently. According to the reported by Cervantes et al. [19], this latter result is controlled by the relative abundance of Ce^{+4}.

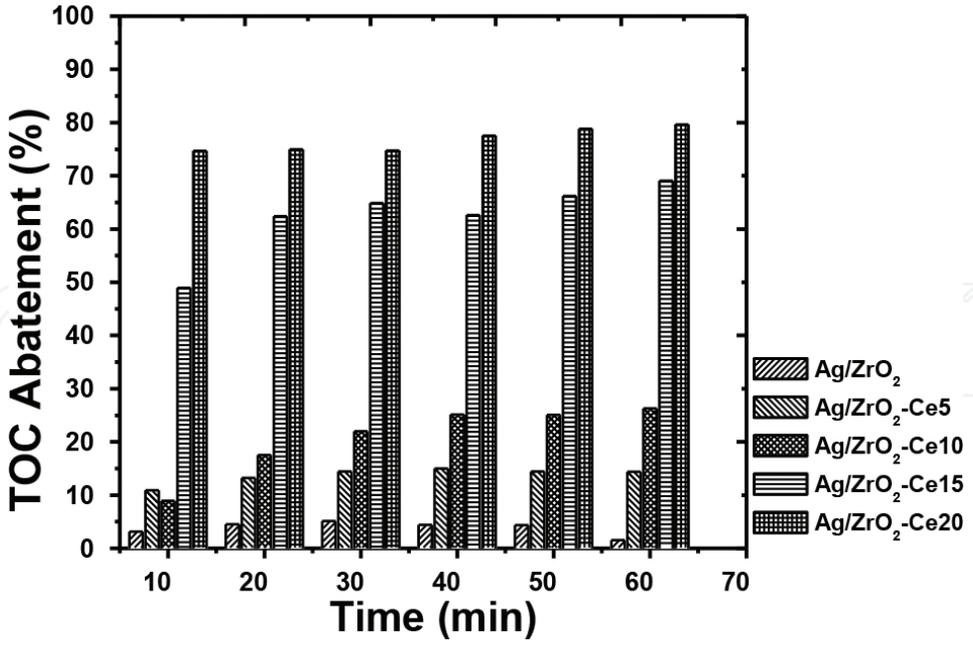


Figure 4. TOC abatement as a function of the time for silver supported catalysts.

This activity results demonstrate the effect of the ceria content on the effectiveness of the MTBE degradation process for the supported Ag nanoparticles. With the characterization studies hydrogen temperature programmed desorption and UV-Vis, we verified the high metal dispersion of the silver when in the materials there was a high concentration of ceria since they reached values of between 49 and 61%, the latter value being assigned to the catalyst Ag/ZrO_2-Ce15.

In this study, it was found that one of the essential steps to carry out the oxidation process by the active phase of the supported silver catalysts is the adsorption of molecular oxygen on the surface of the metallic crystallite. The spectra for reduced Ag/ZrO_2, and several Ag/ZrO_2-Cex containing catalysts it is important to point out that the most intense plasma absorption is for the Ag/ZrO_2-Ce15. This finding suggests that this catalyst should contain the larger proportion of metallic silver. In other words, Ag/ZrO_2-Ce15 has more abundance of Ag^0 nanoparticles compared to their monometallic counterparts. This result shows better performance of chemisorption of oxygen over Ag/ZrO_2-Ce15 and Ag/ZrO_2-Ce20 than the rest of catalyst.

The results of XPS revealed the importance of ceria in the improvement of silver properties. **Figure 5** shows XPS of $Ce_{3d\ 5/2}$ and $Ce_{3d\ 3/2}$ core levels for calcined and H_2-reduced samples and according to several similar studies, the slightly negative shift of Binding Energies was attributed that cerium is mainly in the Ce^{+4} oxidation state, with a certain increase in the Ce^{+3}. For the samples prepared for our study, the $Ce_{3d\ 5/2}$ of Ag/ZrO_2-Ce20 is 0.3 eV smaller than of ZrO_2-Ce20, indicating a greater abundance of Ce^{+3} species, after doping of silver. In this way, we show the presence of oxygen vacancies in the ceria, in the materials with the highest percentage of ceria.

The results showed that in the Ag_{3d} region consisted of two peaks which corresponded to $Ag_{3d\ 5/2}$ and $Ag_{3d\ 3/2}$ and it was determined that The $Ag_{3d\ 5/2}$ binding energies of Ag/ZrO_2 and

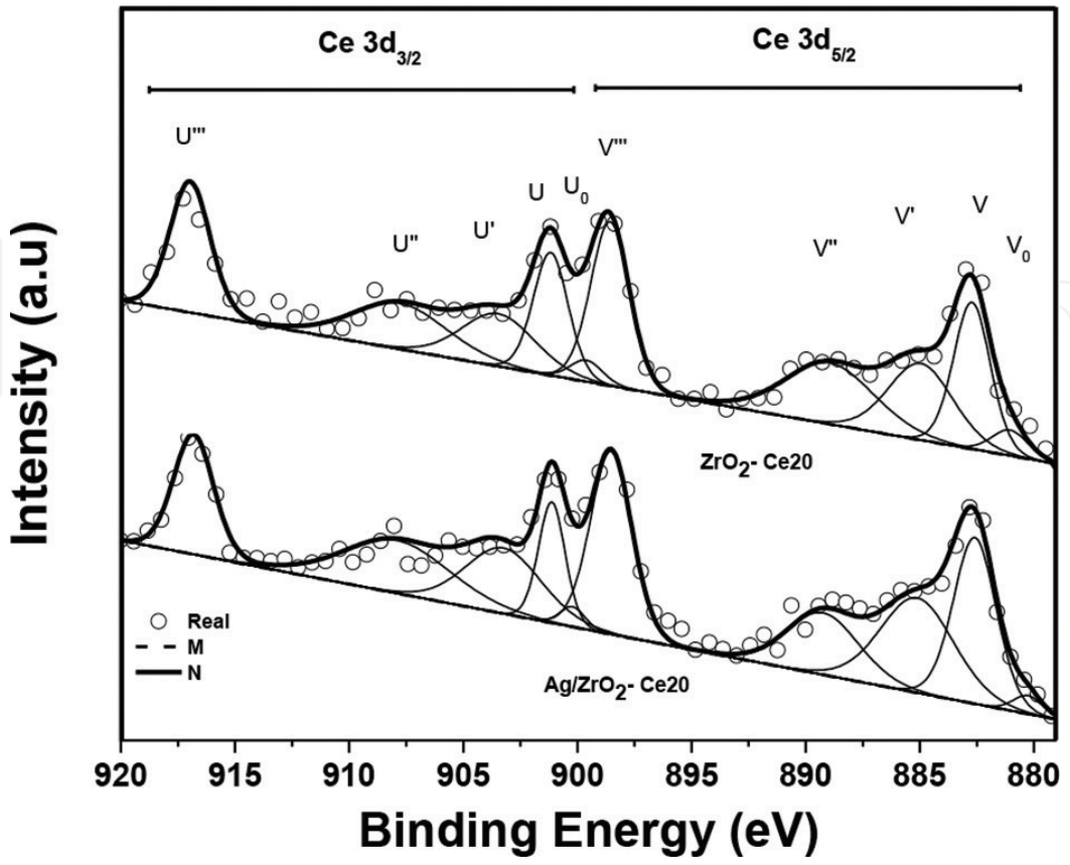


Figure 5. XPS Ce 3D spectra for ZrO_2-Ce20 support and Ag/ZrO_2-Ce20 catalyst.

Ag/ZrO_2-Ce20 were 368.2 and 368.5 eV, respectively. These results demonstrate that only one form of Ag is present, in the form of Ag0. This is because we did not observe any peak corresponding to the oxidized silver species located around 367.7 eV.

The ceria through the oxygen vacancies exerts an interaction between the support and Ag nanoparticles, which allows the silver to become more metallic, increasing the degree of reduction state of silver. This behavior was observed when there is a higher percentage of ceria in the catalysts synthesized, in the case of Ag/ZrO_2-Ce20. That is why the catalysts Ag/ZrO_2-Ce15 and Ag/ZrO_2-Ce20 showed better activity or degradation efficiency of CWAO for MTBE.

With respect to the bimetallic catalysts synthesized by the redox method (Au-Ag/ZrO_2-Cex), CWAO tests were performed under the same conditions presented for the monometallic.

Results from **Table 3** show that on Au-Ag/ZrO_2-Ce5 the MTBE conversion has value 86% and TOC conversion of 68%, being the Au-Ag/ZrO_2-Ce5 the most active catalyst.

Table 3 shows the activity and selectivity for the catalyst Wet-Air Oxidation of MTBE after 60 min of reaction. MTBE conversion (X_C), TOC abatement (X_{TOC}) and intermediate concentration (Acetone) as a function of the time for gold-silver supported catalysts.

Catalysts	X_C (%)[a]	X_{TOC} (%)[a]	C (mmol/l)[a]	r_1[a] (mmol $h^{-1}g_{met}^{-1}$)	Selectivity to CO_2[a]
Ag-Au/ZrO_2	78	61	n.d.	2310	78
Ag-Au/ZrO_2-(5%)CeO_2	86	68	n.d.	2580	79
Ag-Au/ZrO_2-(10%)CeO_2	77	68	n.d.	2340	88
Ag-Au/ZrO_2-(15%)CeO_2	81	59	n.d.	2430	73
Ag-Au/ZrO_2-(20%)CeO_2	86	61	n.d.	2580	71
Without catalyst	51	16	6	—	31

[a]Obtained after 1 h of reaction, n.d. not detected.

Table 3. Activity and selectivity for the catalyst of MTBE after 60 min of reaction.

The values determined by TOC in the MTBE CWAO of bimetallic catalysts, it is observed that the effect of the ceria is minimized, and when depositing the gold (2.5%), it is possible to improve the TOC of Au-Ag/ZrO_2, Au-Ag/ZrO_2-Ce5 and Au-Ag/ZrO_2-Ce10, the opposite being for Au-Ag/ZrO_2-Ce15 and Au-Ag/ZrO_2-Ce20.

The XPS results showed that For the pure Ag/ZrO_2 and Ag/ZrO_2-20% CeO_2, the binding energy (BEs) of $Ag_{3d\ 5/2}$ were 368.243 and 368.355 eV, which is slightly higher than that of bulk metallic Ag (368.1–386.5 eV). Moreover, for the bimetallic catalyst, the BE $Ag_{3d\ 5/2}$ were 368.22 eV for Ag-Au/ZrO_2, 368.23 eV for Ag-Au/ZrO_2-10% CeO_2 and 367.36 eV for Ag-Au/ZrO_2-Ce20. This implies that through allowing gold, the silver has a greater tendency to lose electrons. Therefore, the doping ceria of support affected the degree of reduction of silver in the Ag-Au system. The relative abundance of Ag^0/Ag^{+1} were 49.14/50.86, obtained after deconvolution of Ag_{3d} of Ag-Au/ZrO_2-Ce20.

For the bimetallic catalyst, the XPS analysis of Au_{4f} shifted to slightly higher values compared Ag-Au/ZrO_2 (83.9455 eV) and Ag-Au/ZrO_2-Ce10 (83.9604 eV), but closer to that of the bulk metallic Au (84 eV). But, for the Ag-Au/ZrO_2-Ce20, the BE Au_{4f} was 84.7392 eV. The relative abundance of Au^0/Au^{+1} were 89.74/10.26, obtained after deconvolution of Au_{4f} of Ag-Au/ZrO_2-Ce20. This implies that promoter Ce, in high loading, can inhibit the formation of Ag^0 and Au^0 species, in the bimetallic catalyst. It is because of that the catalyst Au-Ag/ZrO_2-Ce5 shows better activity or degradation efficiency of CWAO for MTBE.

4. Conclusions

The addition of CeO_2 to the ZrO_2 system varied the textural and electronic properties, corroborated by physisorption of N_2 and UV-Vis; increasing the surface area of the support and its capacity of oxide-reduction of the system.

The monometallic nanoparticles by the method deposit precipitation (DP) with NaOH gives excellent results obtaining nanoparticles less than 10 nm, even reaching 2.4 nm for the case

of the material Ag/ZrO_2-Ce20 (M7). The DP method with urea for the bimetals, improved the particle size (2 nm in the B4-U*), although the oxidation is not modified by the size of the nanoparticles.

The addition of Au by the precipitation method with urea modifies the active sites of monometallic material, dispersing the gold in nanometric sizes, not greatly modifying the surface area of the monometallic system, this is corroborated by the TPD-NH_3. The dynamic interaction between Au and CeO_2 modifies the properties of ceria.

For the degradation of phenol, the best catalytic material was Au-Ag/ZrO_2-Ce20 (B7-U*) with a composition of 1.4% Ag and a ratio of Au: Ag molar 1:1 supported in ZrO_2-CeO_2 (20% by weight), due to the strong metal-support interaction that modifies the structure of CeO_2, creating strong acid sites that promote the mineralization of phenol in a catalytic wet oxidation reaction.

A higher percentage of ceria greater vacancies of oxygen and there is an interaction between the support and the silver nanoparticles, allowing the Ag to be reduced to its metallic state. In the monometallic Ag/ZrO_2-CeO_2 catalysts with 5, 10, 15 and 20% ceria, the MTBE conversion was from 52 to 90%; the most active was Ag/ZrO_2-Ce15. The bimetallic catalyst Ag/ZrO_2-Ce5 (B2-R*) was the best in the degradation of CWAO for MTBE, because those containing higher Ce content (Ag-Au/ZrO_2-20% CeO_2) the relative abundance of Au^0/Au^{+1} obtained from the deconvolution of Au_{4f} was 89.74/10.26, which suggests that Ce at high concentrations inhibits the formation of Ag^0 and Au^0 species in bimetallic catalysts.

Author details

Zenaida Guerra Que, José Gilberto Torres Torres, Hermicenda Pérez Vidal*,
María A. Lunagómez Rocha, Juan C. Arévalo Pérez, Ignacio Cuauhtémoc López,
Durvel De La Cruz Romero, Alejandra E. Espinosa De Los Monteros Reyna,
José G. Pacheco Sosa, Adib A. Silahua Pavón and Jorge S. Ferráez Hernández

*Address all correspondence to: hermicenda.perez@ujat.mx

Laboratory of Catalytic Nanomaterials Applied to the Development of Energy Sources and Environmental Remediation, Applied Science and Technology Research Center of Tabasco (CICTAT), Juarez Autonomous University of Tabasco, DACB, Cunduacan, Tabasco, Mexico

References

[1] Gehringer P, Sampa MHO, Ham B, Kim Y, Kim J, Kang H, Shin K, Salimov RA. Status of industrial scale radiation treatment of wastewater and its future. In: Proceedings of a Consultants Meeting of the International Atomic Energy Agency (IAEA); 13-16 October 2003; Daejon, Vienna: IAEA; 2004. pp. 1-18

[2] Wei H, Yan X, He S, Sun C. Catalytic wet air oxidation of pentachlorophenol over Ru/ZrO_2 and Ru/$ZrSiO_2$ catalysts. Catalysis Today. 2013;**201**:49-56

[3] European Commission. 2000. The Water Framework Directive. EC Directive 2000/60/EEC

[4] Glaze WH, Kang JW, Chapin DH. The chemistry of water treatment processes involving ozone, hydrogen-peroxide and ultraviolet-radiation. Ozone: Science & Engineering. 1987;**9**:335-352

[5] Luan M, Jing G, Piao Y, Liu D, Jin L. Treatment of refractory organic pollutants in industrial waste water by wet air oxidation. Arabian Journal of Chemistry. 2017;**10**:S769-S776

[6] Zhou H, Smith DW. Advanced technologies in water and wastewater treatment. Journal of Environmental Engineering and Science. 2002;**1**:247-264

[7] Debellefontaine H, Chakchouk M, Foussard JN, Tissot D, Striolo P. Treatment of organic aqueous wastes: Wet air oxidation and wet peroxideoxidation. Environmental Pollution. 1996;**92**:155-164

[8] Kulkarni SJ, Kaware JP. Review on research for removal of phenol from wastewater. International Journal of Science and Research Publications. 2013;**4**:1-5

[9] Chindris A. Degradation of refractory organic compounds in aqueous wastes employing a combination of biological and chemical treatments [Thesis]. Cagliari: University of Cagliari; 2010

[10] Lin C-W, Cheng Y-W, Tsai S-L. Influences of metals on kinetics of methyl tert-butyl ether biodegradation by *Ochrobactrum cytisi*. Chemosphere. 2007;**69**:1485-1491

[11] Zheng C, Zhao L, Zhou X, Fu Z, Li A. Treatment Technologies for Organic Wastewater. Rijeka, Croatia: In Tech Open; 2013. pp. 249-286

[12] Massa P, Ivorra F, Haure P, Medina Cabello F, Fenoglio R. Catalytic wet air oxidation of phenol aqueous solutions by 1% Ru/CeO_2-Al_2O_3 catalysts prepared by different methods. Catalysis Communications. 2007;**8**:424-428

[13] Kim K-H, Ihm S-K. Heterogeneous catalytic wet air oxidation of refractory organic pollutants in industrial wastewaters: A review. Journal of Hazardous Materials. 2011;**186**:16-34

[14] Shahidi D, Roy R, Azzouz A. Advances in catalytic coxidation of organic pollutants prospects for thorough mineralization by natural clay catalysts. Applied Catalysis, B: Environmental. 2015;**174-175**:277-292

[15] Herney-Ramirez J, Vicente MA, Madeira LM. Heterogeneous photo-Fenton oxidation with pillared clay-based catalysts for waste water treatment: A review. Applied Catalysis, B: Environmental. 2010;**98**:10-26

[16] Li N, Descorme C, Besson M. Application of $Ce_{0.33}Zr_{0.63}Pr_{0.04}O_2$ supported noble metal catalysts in the catalytic wet air oxidation of 2-chlorophenol: Influence of there action conditions. Applied Catalysis, B: Environmental. 2008;**80**:237-247

[17] Delgado JJ, Chen X, Pérez-Omil JA, Rodríguez-Izquierdo JM, Cauqui MA. The effect of reaction conditions on the apparent deactivation of Ce-Zr mixed oxides for the catalytic wet oxidation of phenol. Catalysis Today. 2012;**180**:25-33

[18] Cuauhtémoc I, Del Angel G, Torres G, Lafaye G, Navarrete J, Angeles-Chavez C, Padilla JM. Synthesis and characterization of $Rh/Al2O_3$-CeO_2 catalysts: Effect of the Ce^{+4}/Ce^{+3} ration on the MTBE removal. Journal of Ceramic Processing Research. 2009;**10**:512-520

[19] Cervantes A, Del Angel G, Torres G, Lafaye G, Barbier J Jr, Beltramini JN, Cabañas-Moreno JG, Espinoza de los Monteros A. Degradation of methyl tert-butyl ether by catalytic wet air oxidation over Rh/TiO_2-CeO_2 catalysts. Catalysis Today. 2013;**212**:2-9

[20] Guerra-Que Z, Torres-Torres G, Pérez-Vidal H, Cuauhtémoc-López I, Beltramini JN, Espinoza de los Monteros A, Frías-Márquez DM. Silver nanoparticles supported on zirconia-ceria for the catalytic wet air oxidation of methyl tert-butyl ether. RSC Advances. 2017;**7**:3599-3613

[21] Chen D, Qu Z, Shen S, Li X, Shi Y, Wang Y, Fu Q, Wu J. Comparative studies of silver based catalyst supported on different supports for the oxidation of formaldehyde. Catalysis Today. 2011;**175**:338-345

[22] Shimizu K-I, Kawachi H, Komai S-I, Yoshida K, Sasaki Y, Satsuma A. Carbon oxidation with Ag/Ceria prepared by self-dispersion of Ag power into nano-particles. Catalysis Today. 2011;**175**:93-99

[23] Alabbab S, Adil SF, Assal ME, Khan M, Al warthan A. Gold and silver nanoparticles supported on manganese oxide: Synthesis, characterization and catalytic studies for selective oxidation of benzyl alcohol. Arabian Journal of Chemistry. 2014;**7**:1192-1198

[24] Ruiz-Trejo E, Boldrin P, Medley-Hallam JL, Darr J, Atkinson A, Brandon NP. Partial oxidation of methane using silver/gadolinia-doped ceria composite membranes. Chemical Engineering Science. 2015;**127**:269-275

[25] Almendáres A, González J. Nanomateriales: Su crecimiento, caracterización estructural y tendencias. Ideas CONCYTEG. 2011;**72**:772-787

[26] Salman H, Godlisten N, Imran S, Sung S, Nadir A, Suleman T, Manwar H, Wookeun B, Hee T. Aminated polyethersulfone-silver nanoparticles (AgNPs-APES) composite membranes with controlled silver ion release for antibacterial and water treatment applications. Materials Science and Engineering. 2016;**62**:732-745

[27] Noritomi H, Umezawa Y, Miyagawa S, Kato S. Preparation of highly concentrated silver nanoparticles in reverse micelles of sucrosefatty acid esters through solid-liquid extraction method. Advances in Chemical Engineering and Science. 2011;**1**:299-309

[28] Zhiya S, Joy D, Jizhong Z, Yang L. Contradictory effects of silver nanoparticles on activated sludge wastewater treatment. Journal of Hazardous Materials. 2018;**341**:448-456

[29] Uma P, Fuangfa U. Simultaneous adsorption of silver nanoparticles and silver ions on large pore mesoporous silica. Journal of Environmental Chemical Engineering. 2018;**66**:596-603

[30] Delgado-Beleño Y, Martinez-Nuñez C, Cortez-Valadez M, Flores-López N, Flores-Acosta M. Optical properties of silver, silver sulfide and silver selenide nanoparticles and antibacterial applications. Materials Research Bulletin. 2018;**99**:385-392

[31] Majles M, Dehghani Z, Sahraei R, Nabiyouni G. Non-linear optical properties of silver nanoparticles prepared by hydrogen reduction method. Optics Communications. 2009; **283**:1650-1653

[32] Noginov M, Zhu G, Bahoura M, Adegoke J, Small C, Ritzo B, Drachev V, Shalaev V. The effect of gain and absorption on surface plasmons in metal nanoparticles. Applied Physics B: Lasers and Optics. 2007;**86**:455-460

[33] Wang A, Hsieh Y, Chen Y, Mou C. Au–Ag alloy nanoparticle as catalyst for CO oxidation: Effect of Si/Al ratio of mesoporous support. Journal of Catalysis. 2006;**237**:197-206. DOI: 10.1016/j.jcat.2005.10.030

[34] Liu J-H, Wang A-Q, Chi Y-S, Lin H-P, Mou C-Y. Synergistic effect in an Au-Ag alloy nanocatalyst: CO oxidation. The Journal of Physical Chemistry. B. 2005;**109**:40-43. DOI: 10.1021/jp044938g

[35] Wang J, Zhu W, He X, Yang S. Catalytic wet air oxidation of acetic acid over different ruthenium catalysts. Catalysis Communications. 2008;(13):2163-2167. DOI: 10.1016/j.catcom.2008.04.019

[36] Grunwaldt J, Maciejewski M, Becker OS, Fabrizioli P, Baiker A. Comparative study of Au/TiO_2 and Au/ZrO_2 catalysts for low-temperature CO oxidation. Journal of Catalysis. 1999;**186**:458-469

[37] Schubert M. CO oxidation over supported gold catalysts—"inert" and "active" support materials and their role for the oxygen supply during reaction. Journal of Catalysis. 2001;(1):113-122. DOI: 10.1006/jcat.2000.3069

[38] Wang A, Liu J, Lin S, Lin T, Mou C. A novel efficient Au–Ag alloy catalyst system: Preparation, activity, and characterization. Journal of Catalysis. 2005;**1**:186-197. DOI: 10.1016/j.jcat.2005.04.028

[39] Hayelom D, Adhena A, Hailemariam K, Tekilt G. Synthesis paradigm and applications of silver nanoparticles (AgNPs), a review. Sustainable Materials and Technologies. 2017; **13**:18-23

[40] Akter M, Tajuddin Sikder MD, Mostafizur Rahman MD, AtiqueUllah AKM, Binte Hossain KF, Banik S, Hosokawa T, Saito T, Kurasaki M. A systematic review on silver nanoparticles-induced cytotoxicity: Physicochemical properties and perspectives. Journal of Advanced Research. DOI: 10.1016/j.jare.2017.10.008

[41] Kalantari K, Muhammad Afifi AB, Bayat S, Shameli K, Yousefi S, Mokhtar N, Kalantari A. Heterogeneous catalysis in 4-nitrophenol degradation and antioxidant activities of silver nanoparticles embedded in tapioca starch. Arabian Journal of Chemistry. In press. DOI: 10.1016/j.arabjc.2016.12.0182017

[42] Passos de Aragao A, De Oliveira TM, Veras Queremes P, Gomes Perfeito ML, Carvalho Araújo M, Sousa Santiago JA, Cardoso VS, Quaresma P. Green synthesis of silver nanoparticles using the seaweed *Gracilaria birdiae* and their antibacterial activity. Arabian Journal of Chemistry. In press. DOI: http://dx.doi.org/10.1016/j.arabjc.2016.04.014

[43] Regalbuto J. Catalyst Preparation. Science and Engineering. 2nd ed. CRC Press, Taylor & Francis. 2007. 488 p

[44] García JA, Arreola Sanchez R, Ríos Enríquez MA, Rentería Tapia VM, Valverde Aguilar G. Estudio del desempeño de un catalizador $Au/TiO_2/SiO_2$ en la reaccion de oxidación de CO. Revista Mexicana de Física. México. 2011;**2**:30-35

[45] Redina E, Greish A, Novikov R, Strelkova A, Kirichenko O, Tkachenko O, Kapustin G, Sinev I, Kustov L. $Au/Pt/TiO_2$ catalysts prepared by redox method for the chemo selective 1,2-propanediol oxidation to lactic acid and NMR spectroscopy approach for analyzing the product mixture. Applied Catalysis, A: General. 2015;**491**:170-183

[46] Pieck CL, Marecot P, Barbier J. Preparation of $Pt-Re/Al_2O_3$ catalysts by surface redox reactions. I. Influence of operating variables on Re deposit in the presence of hydrochloric acid. Applied Catalysis, A: General. 1996;**134**:319-329

[47] Astruc D. Nanoparticles and Catalysis. Wiley-VCHVerlag GmbH; 1999

[48] Luck F. Wet air oxidation: Past, present and future. Catalysis Today. USA. 1999;**1**:81-91. DOI: 10.1016/S0920-5861(99)00112-1

[49] Igawa N, Ishii Y. Crystal structure of metastable tetragonal zirconia up to 1473 K. Journal of the American Ceramic Society. 2001;**5**:1169-1171. DOI: 10.1111/j.1151-2916.2001.tb00808.x

[50] Ranga Rao G, Ranjan Sahu H. XRD and UV-Vis diffuse reflectance analysis of CeO_2–ZrO_2 solid solutions synthesized by combustion method. Proceedings of the Indian Academy Of Science. 2001;**5-6**:651-658

[51] Shah A, Qureshi R, Latif-ur R, Synthesis Z-u R. Characterization and applications of bimetallic (Au-Ag, Au-Pt, Au-Ru) alloy nanoparticles. Reviews on Advanced Materials Science. 2012;**30**:133-149

[52] Fu Q, Kudriavtseva S, Saltsburg H, Flytzani-Stephanopoulos M. Gold–ceria catalysts for low-temperature water-gas shift reaction. Chemical Engineering Journal. 2003;**1**:41-53

[53] Rao GR, Fornasiero P, Monte RD, Kašpar J, Vlaic G, Balducci G. Reduction of NO over partially reduced metal-loaded CeO_2–ZrO_2 solid solutions. Journal of Catalysis. 1996;**254**:1-9

[54] Trovarelli A. Catalytic properties of ceria and CeO^{2-} containing materials. Catalysis Reviews. 1996;**4**:439-520. DOI: 10.1080/01614949608006464

[55] Zhang L, Zhang C, He H. The role of silver species on $Ag\ Al_2O_3$ catalysts for the selective catalytic oxidation of ammonia to nitrogen. Journal of Catalysis. 2009;**1**:101-109